

# The effect of absorbed moisture and resin pressure on porosity in autoclave cured epoxy resin

Andrea Dei Sommi<sup>1,2</sup> | Francesca Lionetto<sup>1</sup>  | Giuseppe Buccoliero<sup>1,3</sup> | Alfonso Maffezzoli<sup>1</sup> 

<sup>1</sup>Department of Engineering for Innovation, University of Salento, Lecce, Italy

<sup>2</sup>ENEA, Research Centre of Brindisi, Brindisi, Italy

<sup>3</sup>Advanced Materials and Processes Consulting Department, CETMA, Brindisi, Italy

## Correspondence

Francesca Lionetto, Department of Engineering for Innovation, University of Salento, Via Arnesano, Lecce 73100, Italy.  
Email: [francesca.lionetto@unisalento.it](mailto:francesca.lionetto@unisalento.it)

## Abstract

One of the main issues in epoxy-based composite manufacturing is the formation of porosity derived from moisture absorption during storage and layup due to the high hydrophilicity of epoxy matrices. During the curing process, the presence of moisture and other volatile compounds can initiate the nucleation and growth of voids. In this study, the effect of both the initial water content absorbed in the uncured resin and the pressure on the porosity development in an epoxy resin was investigated. In particular, Kardos' and Ledru's models, aimed at predicting void formation in polymers, were applied to study the effect of different hydrostatic pressures in an epoxy resin during curing up to the gel point, after conditioning it at two different relative humidity levels, 50% and 95%. Subsequently, the porosity of the cured resin samples was quantified through density measurements. Comparative analysis of the microscopy images of cured samples and the predictions of both models revealed an overestimation of the final void sizes by both models, with the Kardos' model exhibiting a higher deviation. Additionally, a finite element model was employed to investigate the conditions leading to void formation, aiming to understand the factors influencing the porosity development and properly set the process parameters during composite manufacturing.

## Highlights

- Evaluation of the conditions leading to void growth in epoxy resin during curing
- Moisture sorption in uncured epoxy resin
- Effect of curing pressure on pore development
- Finite element analysis for void growth during resin curing

## KEYWORDS

autoclave, composites, epoxy resin, finite element analysis, moisture sorption, porosity, void growth

This is an open access article under the terms of the [Creative Commons Attribution-NonCommercial](https://creativecommons.org/licenses/by-nc/4.0/) License, which permits use, distribution and reproduction in any medium, provided the original work is properly cited and is not used for commercial purposes.

© 2024 The Author(s). *Polymer Composites* published by Wiley Periodicals LLC on behalf of Society of Plastics Engineers.

## 1 | INTRODUCTION

Epoxy resins find many applications, including paints and coatings, adhesives, electronic materials, biomedical systems, and matrices for fiber-reinforced composites due to their high mechanical properties, adhesion strength, thermal stability, and dielectric behavior.<sup>1,2</sup> Epoxy-based composites can be processed through many technologies, from liquid composite molding (LCM) processes to filament winding (FW) and autoclave or out-of-autoclave (OoA) layup.<sup>3–8</sup> Autoclave lamination, based on the use of pre-impregnated unidirectional carbon fiber tapes (the so-called prepregs), is the process adopted by the aeronautic industry for manufacturing high-performance fiber-reinforced composite parts, with severe quality requirements.<sup>9</sup> Prepreg materials containing epoxy resins are sensitive to moisture absorption during storage and lamination,<sup>10,11</sup> which leads to the development of porosity during the curing process of resin.<sup>12–15</sup> Multiple vacuum bagging (debulking) is usually applied in clean room lamination to consolidate the laminate and remove entrapped air, making the porosities arising from water or other volatile compounds the main issue. To avoid or limit this detrimental phenomenon responsible for property reduction eventually leading to part rejection,<sup>16–20</sup> it is possible to properly set the process parameters, mainly pressure and temperature.<sup>21–27</sup>

Several models are available in the literature for predicting void growth, content, and size. The thermodynamic and diffusion aspects of the stability of bubbles in liquid–gas solutions were described in 1950 by Epstein and Plesset.<sup>28</sup> Amon and Denson<sup>29</sup> introduced a model to describe the bubble growth during the foaming of polymeric liquids, afterward modified by Arefmanesh et al.<sup>30,31</sup> and Roychowdhury et al.,<sup>32</sup> who applied the model to amorphous thermoplastic polymers. Kardos et al.<sup>33,34</sup> developed a model to characterize the time-dependent void growth and stability during the cure cycle of composite laminates, where the liquid resin is subjected to pressure and temperature changes of 100–150°C. This model was applied by Boey and Lye<sup>14,35</sup> to predict the final void content in composites. Wood and Bader<sup>36</sup> improved Epstein and Plesset's model by including the effect of surface tension forces on void growth, while Gu et al.<sup>37</sup> improved Kardos' model by considering an air–water vapor mixture void. However, it has been proven that the difference in the minimum resin pressure required to prevent void growth predicted by Kardos' and Gu's models is almost negligible.<sup>38</sup> Ledru et al.<sup>39</sup> presented a coupled visco-mechanical and diffusion model for void growth prediction during composite curing. This model was successfully applied by Wang et al.<sup>40</sup> to FW composites along with a resin flow submodel for fiber volume fraction modeling. Sul et al.<sup>41</sup> studied the bubble formation and

growth phenomena in a polymeric resin when a vacuum is applied. Anderson and Altan<sup>42</sup> proposed a model for void content capable of predicting an asymptotic non-zero value compared with Boey and Lye's model. de Parscau du Plessix et al.<sup>43</sup> proposed the existence of a boundary layer around the bubble with different diffusive properties to explain the slowdown of water diffusion at the bubble interface. More recently, Kermani et al.<sup>44</sup> developed a model for bond-line porosity prediction in honeycomb core sandwich structures. Dei Sommi et al.<sup>23</sup> implemented a model to evaluate the effect of process parameters on porosity development in autoclave cured composites. However, all the reported models are generally unable to predict the actual void size and content and they neglect phenomena like void transport and void coalescence.

In this work, the effect of initial water content absorbed in the uncured resin and of hydrostatic resin pressure on the porosity development in an epoxy resin used for high-performance composites for aeronautical components has been analyzed. The results of this study can be exploited to properly set the process parameters during composite manufacturing. Kardos et al.'s<sup>33</sup> and Ledru et al.'s<sup>39</sup> models have been compared to evaluate the void growth in neat epoxy resin samples. Resin samples have been exposed to a moist environment and then cured under different pressures. The effect of moisture absorption and applied pressure on porosity has been assessed through density and optical microscopy measurements.

## 2 | EXPERIMENTAL

The epoxy resin analyzed in this work was CYCOM<sup>®</sup> 977–2 (Solvay). Its curing kinetics was studied by differential scanning calorimetry (DSC) using a Mettler Toledo DSC 822 calorimeter with dynamic runs on uncured resin from 25 to 300°C at 0.5, 0.75, 1, and 2°C/min in a nitrogen atmosphere. The rheological analysis of the resin was performed on a parallel plate (diameter 25 mm) rheometer (ARES, Rheometrics Scientific) in dynamic mode at 1 Hz from 50 to 200°C at 0.5, 0.75, 1, and 2°C/min. For both analyses, three replicates were performed at each heating rate.

Flat resin samples with a diameter of 50 mm and a thickness of 2 mm were conditioned by exposure to relative humidity (RH) levels of 50% and 95% at a temperature of 25°C until saturation using a Binder KMF 115 climate chamber. RH = 50% represented the typical RH content in clean rooms where lamination of composites for aeronautics is generally performed. A total of 95% RH was adopted either as a reference or to simulate bad storage and handling practices of prepregs. Then, the samples were cured in an oven (Carbolite LHT 6/120) inside a

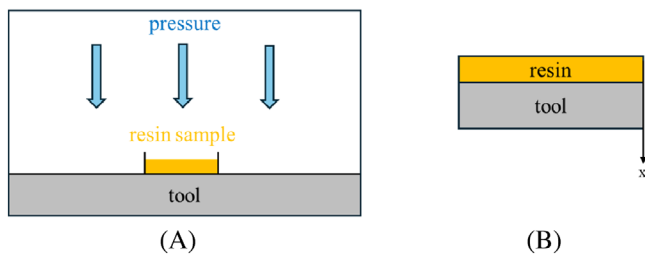


FIGURE 1 Sketch of (A) the adopted experimental setup for each experimental condition and (B) the model domain.

proper custom-made tool with compressed air to simulate the autoclave conditions. Three pressure levels (0.1, 0.2, and 0.5 MPa) were adopted. The curing conditions consisted of a heating stage at 2°C/min up to 180°C and a dwell stage of 3 h at 180°C, as recommended by the prepreg provider. Cured samples were fractured, and the fracture surfaces were analyzed under an optical microscope (Dino-Lite plus, IDCP B.V.). The porosity of three samples for each conditioning process was measured by density measurements according to the ASTM D792 standard.<sup>45</sup> The adopted experimental setup is represented in Figure 1A.

FlexPDE-8 Finite Element (FE) solver (PDE Solutions Inc.) was used to solve the partial and ordinary differential equations for void growth, energy balance, mass diffusion, and reaction kinetics.

### 3 | VOID GROWTH MODELING

#### 3.1 | Kardos' model

The need for a better understanding of porosity development in high-performance composites dates back to the '80s when Kardos et al.<sup>33</sup> developed a model for void growth prediction in composite laminates based on the assumption of spherical pure water voids in an infinite isotropic medium with uniform temperature and moisture concentration. Kardos's model assumed that when the hydrostatic resin pressure is lower than the water vapor pressure, water diffuses into preexisting voids leading to void expansion. Void transport and interaction, water desorption, and surface tension, inertial, and viscous effects are neglected. It is possible to determine the value of void radius  $r$  from the following equation:

$$r = 2 \times \frac{C_{\infty} - C_{\text{sat}}}{\rho_g} \times \sqrt{D \times t}, \quad (1)$$

where  $\rho_g$  (kg/m<sup>3</sup>) is the water vapor density,  $D$  (m<sup>2</sup>/s) is the diffusivity of water in the resin,  $t$  (s) the time,  $C_{\infty}$  and

$C_{\text{sat}}$ , both expressed in kg/m<sup>3</sup>, are the water concentrations in the bulk resin and at the void surface, respectively.

$$C_{\infty} = c_1 \times RH^2, \quad (2)$$

$$C_{\text{sat}} = c_2 \times e^{\frac{9784}{T}} \times P^2, \quad (3)$$

where  $c_1$  (kg/m<sup>3</sup>) and  $c_2$  (kg/m<sup>3</sup>) are two constants, RH (%) is the relative humidity,  $T$  (K) is the absolute temperature, and  $P$  (atm) is the hydrostatic resin pressure. The dependence of  $D$  and  $\rho_g$  on the temperature is expressed by the following equations:

$$D = D_0 \times e^{-\frac{E_a}{R \times T}}, \quad (4)$$

$$\rho_g = \frac{M_{\text{H}_2\text{O}} \times P}{R \times T}, \quad (5)$$

where  $D_0$  (m<sup>2</sup>/s) is a pre-exponential constant,  $E_a$  (J/mol) is the activation energy for diffusion per mole,  $R$  (J/(mol K)) is the universal gas constant, and  $M_{\text{H}_2\text{O}}$  (kg/mol) is the water molecular weight.

The initial value of the void radius is assumed to be zero by Kardos' model.<sup>33</sup> The condition for void growth is  $C_{\text{sat}} < C_{\infty}$ .

Since the study is focused on a resin undergoing to a polymerization reaction, in this work, Kardos' model has been coupled with the kinetic (Equations 6–8) and rheological models (Equation 9) of the curing resin and the energy balance (Equation 10), to evaluate the change in resin degree of reaction  $\alpha$  (–) and viscosity  $\eta$  (Pa s) and the temperature evolution during the exothermic reaction of resin:

$$\frac{d\alpha}{dt} = k_1 \times (\alpha_{\text{max}} - \alpha)^{n_1} + k_2 \times \alpha^m \times (\alpha_{\text{max}} - \alpha)^{n_2}, \quad (6)$$

$$\alpha_{\text{max}} = p + q \times T, \quad (7)$$

$$k_i = k_{0i} \times e^{-\frac{E_{bi}}{R \times T}}, i = 1, 2, \quad (8)$$

$$\eta = \eta_{g0} \times e^{\left[ \frac{G_1 \times (T - T_{g0})}{G_2 + T - T_{g0}} \right] \times \left( \frac{a_g}{a_g - \alpha} \right)^{A+B \times \alpha}}, \quad (9)$$

$$\rho_r \times c_r \times \frac{\partial T}{\partial t} = k_r \times \frac{\partial^2 T}{\partial x^2} + \rho_r \times \Delta h_{\text{ref}} \times \frac{d\alpha}{dt}, \quad (10)$$

where  $m$  (–),  $n_1$  (–), and  $n_2$  (–) are reaction orders,  $k_1$  (s<sup>–1</sup>) and  $k_2$  (s<sup>–1</sup>) are kinetic constants,  $p$  (–) and  $q$  (K<sup>–1</sup>) are two fitting parameters,  $k_{0i}$  (s<sup>–1</sup>) is a pre-exponential

factor,  $E_{bi}$  (J/mol) is the apparent activation energy,  $\eta_{g0}$  (Pa s) is the viscosity of the unreacted resin at the initial glass transition temperature  $T_{g0}$  (K),  $\alpha_g$  (–) is the degree of reaction at gel temperature,  $\rho_r$  (kg/m<sup>3</sup>) is the resin density,  $c_r$  (J/(kg K)) is the resin specific heat,  $k_r$  (W/(m K)) is the resin thermal conductivity in the through-the-thickness direction  $x$  (m),  $\Delta h_{ref}$  (J/kg) is the heat generated by the chemical reaction, and  $A$  (–),  $B$  (–),  $G_1$  (–), and  $G_2$  (K) are other parameters.

The model domain is sketched in Figure 1B. The boundary and initial conditions refer to the curing conditions of the samples, including forced air convection on the upper side of the resin and the presence of the tool on the bottom side.

### 3.2 | Ledru's model

After many attempts in the literature to improve Kardos' model, as described above, Ledru et al.<sup>39</sup> implemented a void growth model that takes into account the effect of gas expansion and water diffusion along with surface tension and viscosity change during resin curing. In this case, water vapor partial pressure is considered (assumption of air–water vapor mixture in the voids). The governing equations of the model are as follows:

$$\frac{d}{dt} \left[ \frac{M_{gas}}{T} \times P_{gas} \right] = 3 \times R \times D \times (C_{\infty} - C_{sat}) \times r \times \left( 1 + \frac{r}{\sqrt{\pi \times D \times t}} \right), \quad (11)$$

$$C_{\infty} = \psi \times \frac{a \times \varphi^b \times \rho_r}{100 \times w_r}, \quad (12)$$

$$C_{sat} = \begin{cases} \psi \times \frac{a \times \rho_r}{100 \times w_r} \times \left( \frac{100 \times x_{H_2O} \times P_{gas}}{P_{sat}} \right)^b, & x_{H_2O} \times P_{gas} < P_{sat} \\ \psi \times \frac{a \times \rho_r}{100 \times w_r} \times (100)^b, & x_{H_2O} \times P_{gas} \geq P_{sat} \end{cases}, \quad (13)$$

$$P_{gas} = P + \frac{4}{r} \times \left( \frac{\gamma}{2} + \eta \times \frac{dr}{dt} \right), \quad (14)$$

$$P_{sat} = P_{sat}^{ref} \times \left( \frac{T_{ref}}{T} \right)^{\frac{\beta}{R}} \times e^{\frac{E_c}{R} \times \left( \frac{1}{T_{ref}} - \frac{1}{T} \right)}, \quad (15)$$

where  $M_{gas}$  (kg/mol) is the gas (air–water vapor mixture) molecular weight,  $P_{gas}$  (Pa) is the gas pressure,  $\varphi$  (%) is the relative humidity,  $w_r$  (–) is the resin weight fraction,  $x_{H_2O}$  (–) is the water mole fraction,  $\gamma$  (N/m) is the surface

tension,  $P_{sat}$  (Pa) is the saturated water vapor pressure,  $P_{sat}^{ref}$  (Pa) is the saturated water vapor pressure at reference temperature  $T_{ref}$  (K), and  $\psi$  (–),  $a$  (–),  $b$  (–),  $\beta$  (J/(mol K)), and  $E_c$  (J/mol) are other parameters. In this case, as well the Ledru's model was associated with Equations (6–10) to account for temperature gradients and the effect of the degree of reaction and temperature on viscosity. Surface tension was assumed constant. The initial void radius for Ledru's model is assumed to be 10  $\mu$ m.<sup>39</sup>

## 4 | RESULTS AND DISCUSSION

The results of rheological and DSC analysis are shown in Figure 2 for a heating rate of 2°C/min, the same indicated in the technical datasheet and used in the FE model. The fitting of experimental DSC and rheological curves at four heating rates was performed according to Equations (6–9),<sup>46,47</sup> and the fitting parameters are also reported in Figure 2.

In the adopted experimental set-up water desorption is potentially allowed but it could be not sufficient to remove completely the absorbed moisture. However, as discussed below, the moisture concentration is high enough for the development of voids. Moreover, although in an autoclave curing cycle, the hydrostatic pressure in the resin is usually lower than the gas pressure in the autoclave,<sup>23</sup> in this set-up the hydrostatic resin pressure  $P$  is equal to the autoclave gas pressure  $P_{aut}$ , since there is no reinforcement or breather and other auxiliary vacuum bagging materials. This assumption was also adopted by some of the aforementioned models, although applied to composite laminates,<sup>33,39,43</sup> while other models tried to account for the effect of reinforcement.<sup>23,40,42</sup> Additionally, compared with neat resin, in composite materials, the assumption of spherical voids is unrealistic since the void nucleation is heterogeneous rather than homogeneous being caused by the presence of fibers.<sup>12,41</sup> The possible nucleation effects of the fibers may be ascribed to their lower surface energy compared with the bulk matrix and their roughness and surface functional groups. Therefore, fibers may provide favorable sites for void formation and growth during the curing process that can become trapped at the fiber–matrix interface. Micro-computed tomography (micro-CT) has demonstrated that porosities in composite laminates present elongated shapes and are aligned to the fibers.<sup>23,48–50</sup> In the present work, which is focused only on the neat resin in the absence of the fibers, the assumption of homogenous nucleation and spherical voids may still be acceptable.

The values of the input parameters of Kardos' and Ledru's models are listed in Table 1. The values for parameters  $c_1$  and  $c_2$  in Equations (2) and (3), respectively, were

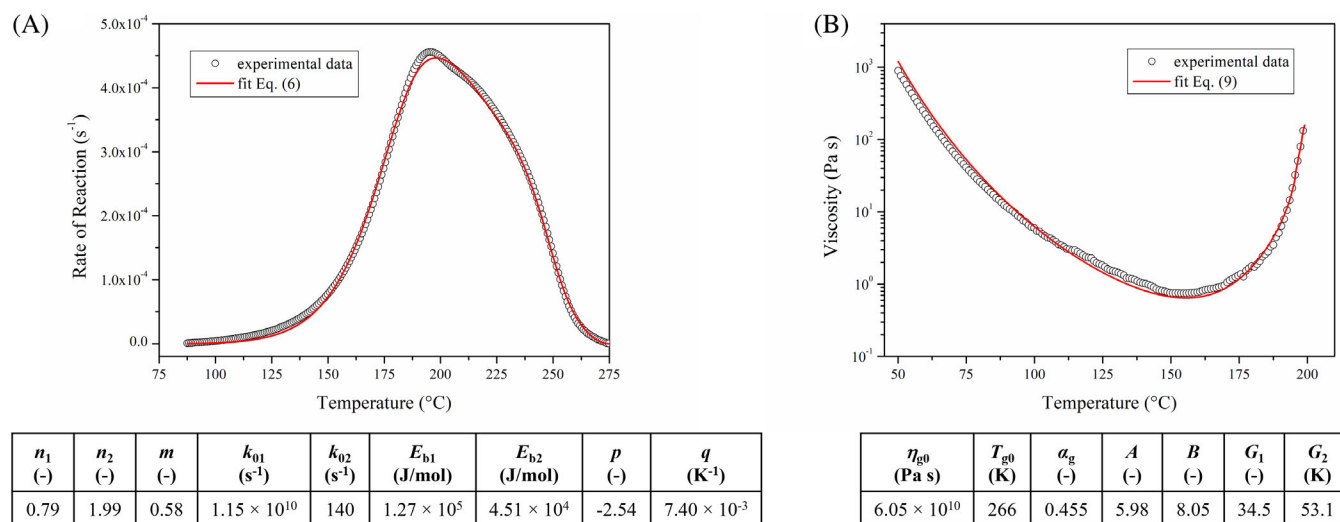


FIGURE 2 (A) Kinetic and (B) rheological modeling of differential scanning calorimetry and rheological analysis at 2°C/min. The fitting parameters are reported below the experimental curve.

TABLE 1 Input parameters used in the void growth models.

$c_1$ (kg/m <sup>3</sup> )	$c_2$ (kg/m <sup>3</sup> )	$D_0^{23}$ (m <sup>2</sup> /s)	$E_a^{23}$ (J/mol)	$M_{H_2O}$ (kg/mol)	$w_r$ (-)
$2.03 \times 10^{-3}$	$8.24 \times 10^{-11}$	$4.61 \times 10^{-2}$	$5.55 \times 10^4$	$1.80 \times 10^{-2}$	1.00
$\rho_r^{52}$ (kg/m <sup>3</sup> )	$c_r^{52}$ (J/(kg K))	$k_r^{52}$ (W/(m K))	$\Delta h_{ref}^{23}$ (J/kg)	$\psi^{39}$ (-)	$\alpha^{39}$ (-)
$1.31 \times 10^3$	$1.10 \times 10^3$	0.17	$3.56 \times 10^5$	0.90	$2.00 \times 10^{-4}$
$b^{39}$ (-)	$\gamma^{39}$ (N/m)	$P_{sat}^{ref39}$ (Pa)	$T_{ref}^{39}$ (K)	$\beta^{39}$ (J/(mol K))	$E_c^{39}$ (J/mol)
1.70	0.05	$3.17 \times 10^3$	298	43.9	$5.71 \times 10^4$

determined through absorption tests on the resin. Although water sorption in liquids should follow an ideal behavior governed by Henry's law, Figure 3 shows an upward curvature typical of a Flory-Huggins behavior.<sup>51</sup> This could be the consequence of high chemical affinity to the water of unreacted resin, which is rich in primary and secondary amines and hydroxyls. This result is also consistent with a power law fit as expected for pure resins. Indeed, the exponent of the power law is 1.8, as reported by Gillet et al.<sup>11</sup>

The FE simulations were stopped at the gel point, when resin becomes rubbery, and viscosity increases enough to stop any possible resin flow and to prevent any further void growth. As determined by rheological analysis, the gel point for this resin heated at 2°C/min was around 150 min, which was also the simulated time in the FE model. The maximum values of void radius predicted by Kardos' ( $r_K$ ) and Ledru's ( $r_L$ ) models, the actual void radius, and the porosity measured by density measurements are listed in Table 2. The values of the predicted void radius and measured porosity as a function of

moisture exposure level and applied pressure are represented in Figure 4A,B, respectively. As expected, the void radius and the actual porosity decrease when a higher pressure is applied, or the samples are exposed to a less moist environment. The trend of porosity is the same observed by Gu et al.,<sup>37</sup> who studied the effects of pressure on the porosity of cured epoxy and bismaleimide resins after conditioning at 50 and 90 %RH. However, the void growth models, when they are applied to neat resin, produce very large pore sizes (except for Ledru's model at RH = 50% and  $P_{aut} = 0.5$  MPa, which predicts no growth), failing to predict the actual void dimension. The micrographs of the cured resin samples are reported in Figure 5. It is worth noting that the mean value of the actual void size is of the same order of magnitude for all conditions. This could be explained by void transport and coalescence phenomena not considered in these models. Voids coalescence is likely to occur when low pressure and high RH exposure are used, as shown in Figure 5. It must be noted that water vapor pressure upon heating at 2°C/min becomes higher than 0.1, 0.2, and 0.5 MPa at

$T = 100, 120,$  and  $150^{\circ}\text{C}$ , respectively. Therefore, the kinetic of void nucleation must play a role considering the very low amount of porosity found when 0.5 MPa is

used. Furthermore, the available models assume that pre-existing voids increase their size, a hypothesis not always reasonable, such as in the neat resin samples here considered, but also in composite laminates after proper debulking cycles. Note that even the highest pressure used in an autoclave, that is, 0.8 MPa, is lower than water vapor pressure when a curing temperature of  $180^{\circ}\text{C}$  is required, confirming that low porosity composites can be obtained even if the thermodynamic condition for void nucleation and growth is satisfied.

Figure 6 shows the time dependence of the ratio  $r/r_0$  of void radius to the initial radius as predicted by the models at the tool side of resin samples along with resin viscosity and autoclave temperature. Both Kardos' and Ledru's models overestimated the void growth, but the latter is more effective since its results are of the same order of magnitude as Roychowdhury et al.'s,<sup>32</sup> who evaluated the moisture or other volatile-induced void formation in thermoplastic polymers as a function of several parameters, including applied pressure. Compared with Kardos' model, Ledru's model is more complete because it includes the effects of resin surface tension and viscosity.

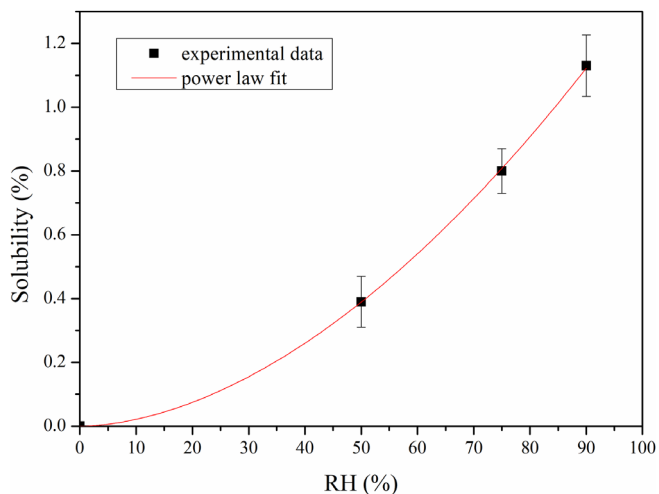


FIGURE 3 Moisture content as a function of relative humidity with power law fit.

RH (%)	$P_{\text{aut}}$ (MPa)	$r_K$ (mm)	$r_L$ (mm)	$r_a$ (mm)	Porosity (%)
50	0.1	205	24.0	$0.29 \pm 0.11$	$27.26 \pm 3.4$
	0.2	99.9	14.0	$0.27 \pm 0.11$	$4.39 \pm 0.70$
	0.5	6.46	$7.41 \times 10^{-3}$	$0.20 \pm 0.15$	$0.21 \pm 0.03$
95	0.1	1010	68.1	$0.62 \pm 0.23$	$32.11 \pm 4.0$
	0.2	491	38.7	$0.36 \pm 0.08$	$11.37 \pm 1.9$
	0.5	154	15.5	$0.29 \pm 0.13$	$0.29 \pm 0.04$

TABLE 2 Predicted void radius by Kardos' ( $r_K$ ) and Ledru's ( $r_L$ ) models, measured void radius ( $r_a$ ), and porosity.

Abbreviation: RH, relative humidity.

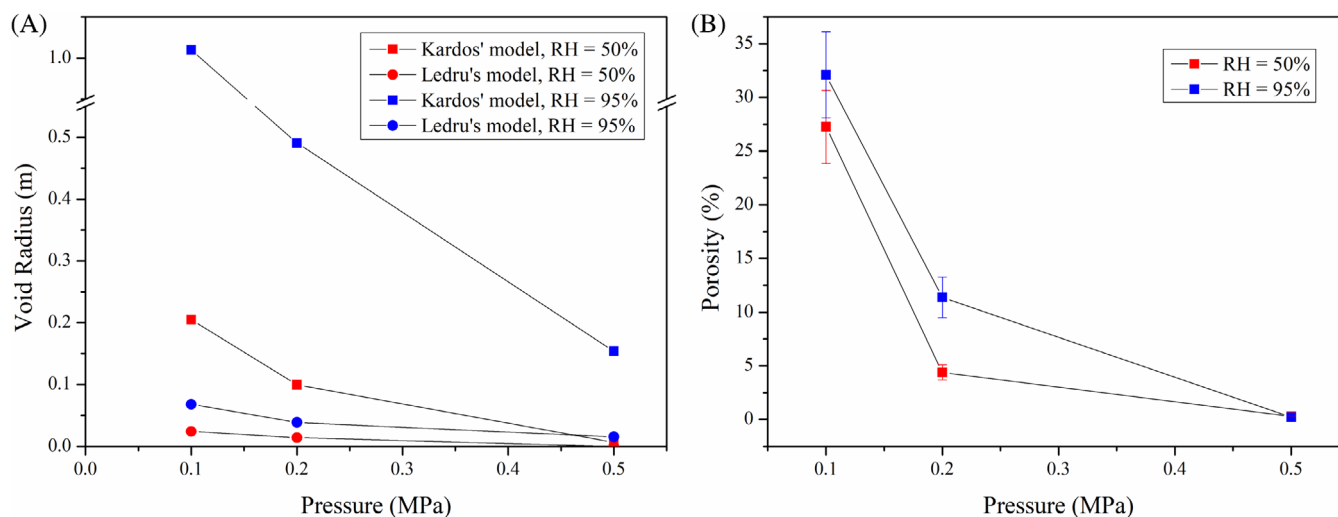


FIGURE 4 (A) Predicted void radius and (B) measured porosity as a function of moisture exposure level and applied pressure. RH, relative humidity.

FIGURE 5 Micrographs of cured resin samples (magnification 25×) at three pressure levels (0.1, 0.2, and 0.5 MPa) after conditioning at two relative humidity (RH) levels (50% and 95%).

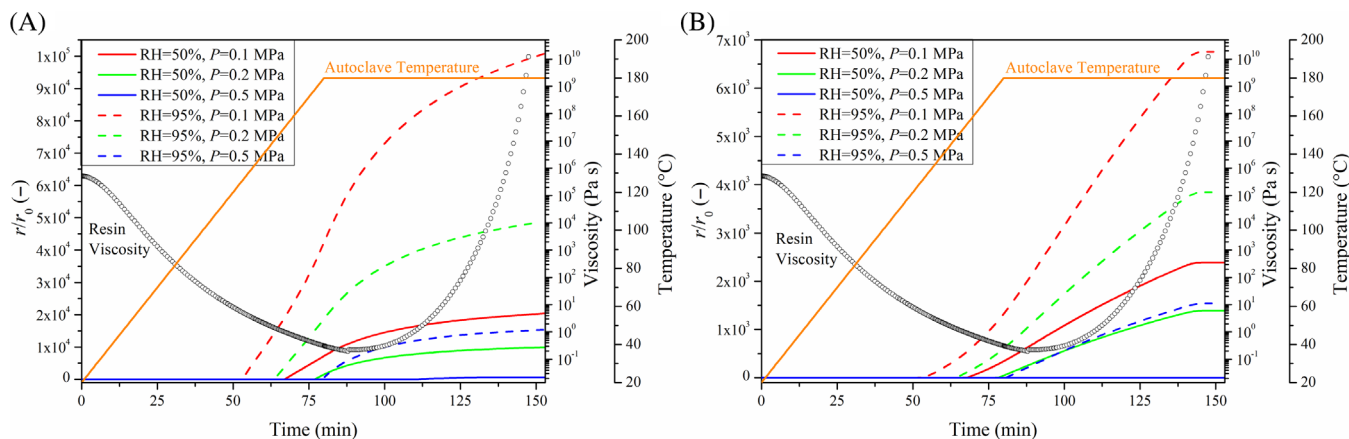
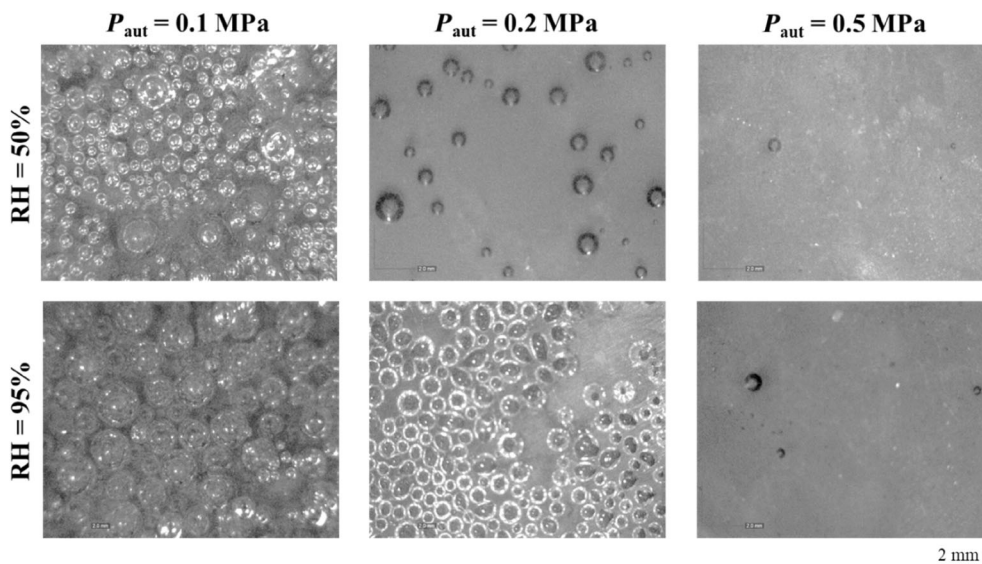


FIGURE 6 Time dependence of autoclave temperature, resin viscosity, and the ratio of void radius to initial radius as predicted by (A) Kardos' and (B) Ledru's models at the tool side of resin samples.

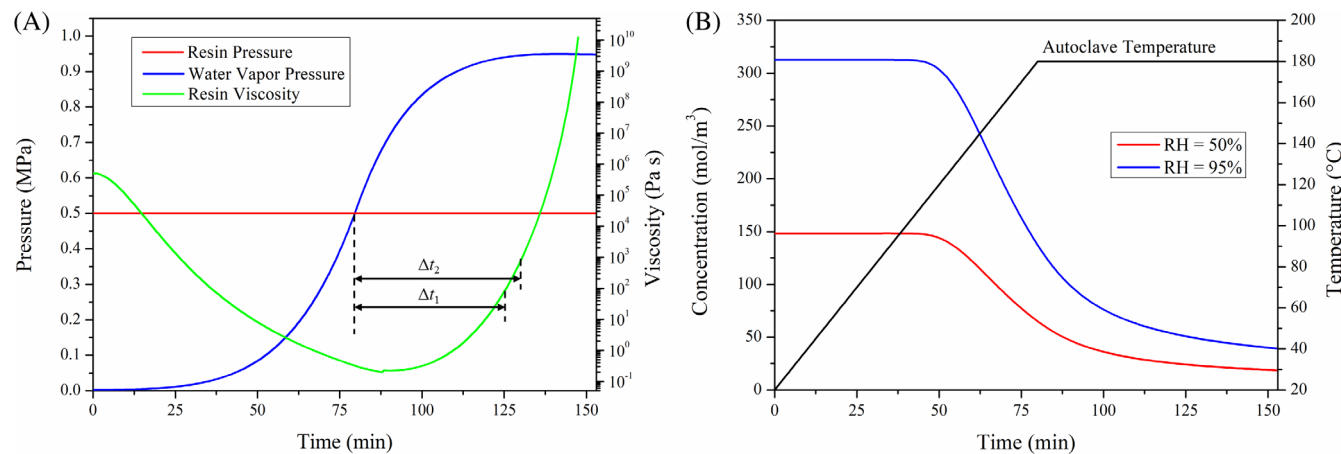


FIGURE 7 Time dependence of (A) resin viscosity and resin and water vapor pressure and of (B) gas temperature and moisture concentration at the tool side of resin samples conditioned at 50% and 95% relative humidity (RH).

Viscosity change, in particular, leads to a plateau in  $r/r_0$  as the resin approaches gelation, as expected.

The adopted conditions are likely to be the same in autoclave curing cycles of composite laminates where the hydrostatic resin pressure is lower than the autoclave pressure because of the presence of the reinforcement and vacuum bagging auxiliary materials.<sup>23</sup> Therefore, the actual hydrostatic resin pressure can be calculated based on the consolidation behavior of the selected reinforcement, as proved in previous work,<sup>23</sup> where a multiphysic model able to predict the potential conditions for porosity development in composite materials was developed.

**TABLE 3** Time intervals for the potential development of voids.

$P_{\text{aut}}$ (MPa)	$\Delta t_1$ (min)	$\Delta t_2$ (min)
0.1	73.3	78.3 (+5)
0.2	62.5	67.5 (+5)
0.5	46.1	51.1 (+5)
0.8	29.4	34.4 (+5)

The overestimation of void size and porosity can be attributed to Kardos' and Ledru's assumption of constant moisture concentration, neglecting water desorption through the breather during the curing cycle. The proposed model<sup>23</sup> only predicts the conditions leading to a resin pressure lower than water vapor pressure. However, this model can be also applied to calculate the time intervals  $\Delta t$  (s) in the curing cycle during which the conditions leading to potential void growth are satisfied. Figure 7A and Table 3 report these time intervals.  $\Delta t_1$  and  $\Delta t_2$  are the time intervals during which water vapor pressure is higher than resin pressure until viscosity is lower than 100 and 1000 Pa s, respectively, which are commonly used for indicating the practical occurrence of gelation, that is, the impossibility of any flow under the used pressure.

The results of the proposed model clearly evidence that the time interval at which the liquid resin is in conditions favorable to void growth decreases as resin pressure increases. This outcome agrees with the low porosity contents achieved with increased resin pressure, as shown in Table 2. However, void growth is still possible

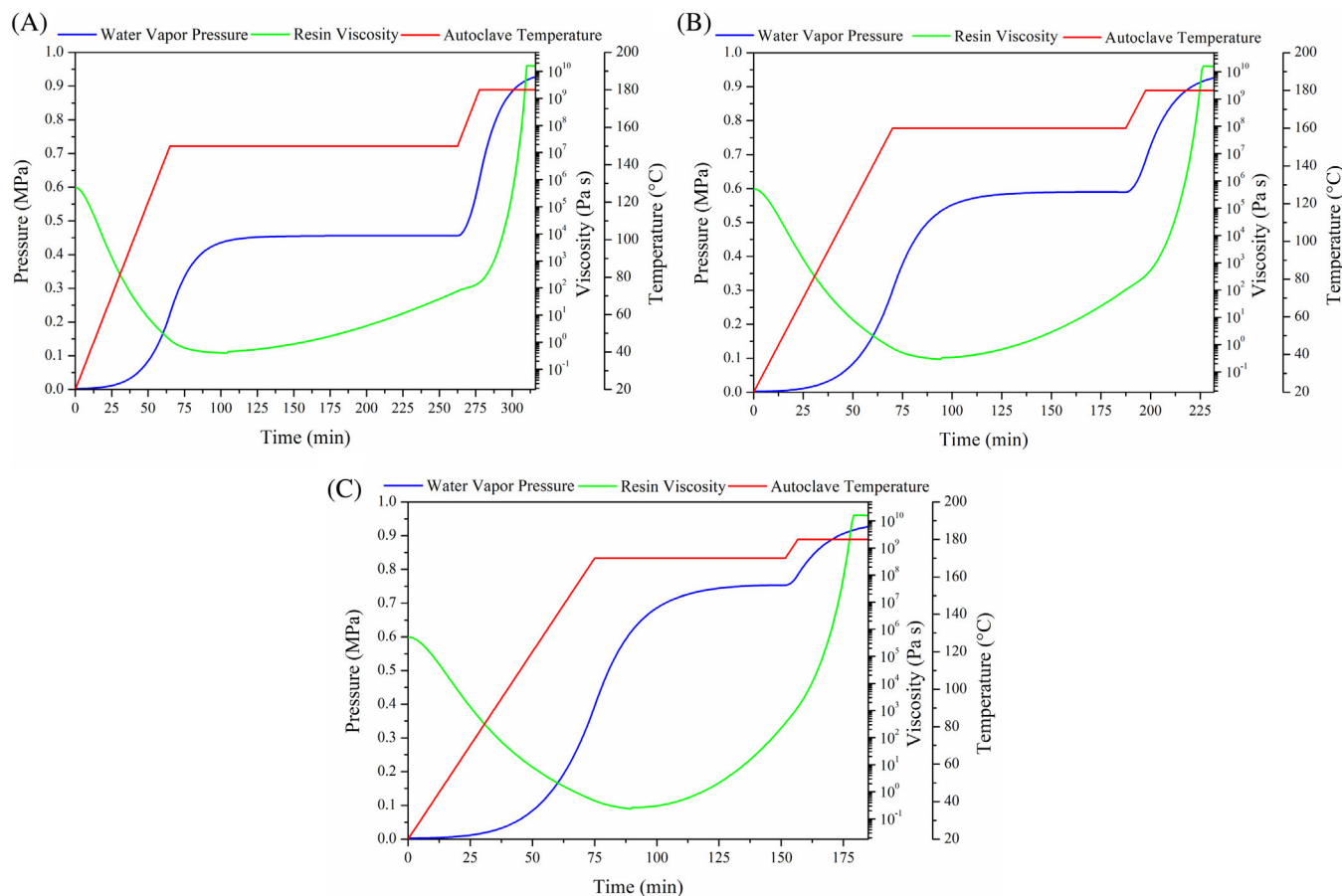


**FIGURE 8** Time dependence of resin viscosity, gas temperature in autoclave, and water vapor pressure at the tool side of resin samples with a  $T_{\text{dwell}}$  of (A) 150°C, (B) 160°C, and (C) 170°C.



at high pressure due to the presence of residual moisture, as determined by Fick's second law of diffusion<sup>53</sup> for a sample conditioned at RH = 50% and 95% and cured under vacuum (Figure 7B). However, the actual process conditions in compressed moist air would restrict water desorption. Even at 0.8 MPa,  $\Delta t_1$  and  $\Delta t_2$  are around 30 min, so there is time for void growth until gelation. Figure 7A shows that a resin pressure close to 1 MPa would be required to completely prevent any potential void growth when a curing temperature of 180°C is required, but this is not feasible since 0.8 MPa is generally not exceeded in autoclaves. This confirms that the proposed model of void growth needs to be combined with a model of void nucleation, which is likely to be heterogeneous in composite laminates where fiber content is between 50% and 65%.

The proposed model can be applied to modify the resin cure cycle to limit the time intervals where there is a real risk of void nucleation and growth. To this aim, a dwell stage at different temperatures ( $T_{\text{dwell}}$ ) until resin gelation has been simulated in the model (Equations 6–10) and its effect on the water vapor pressure curve is reported in Figure 8. Although the cure time is longer than in the absence of the dwell stage, the water vapor pressure is always less than 0.5, 0.6, and 0.8 MPa when adopting a  $T_{\text{dwell}}$  of 150, 160, and 170°C, respectively.

## 5 | CONCLUSION

In this study, the phenomenon of void formation in curing epoxy resins was analyzed. Uncured epoxy resin samples were conditioned at two moisture levels (50 % RH and 95 %RH) and then cured under different pressures (0.1, 0.2, and 0.5 MPa). Kardos' and Ledru's void growth models were applied to estimate the void size at the end of curing. The porosity, determined by density measurements, and the predicted void radii decreased when a higher pressure was applied. However, the predicted radius values were higher than the actual void sizes for both models. Ledru's model was more accurate than Kardos' model as it considers the effects of resin surface tension and viscosity. The overestimation of void size was ascribed to Kardos' and Ledru's assumption of constant moisture concentration, neglecting water desorption during the curing cycle, and lacking a void nucleation kinetic step, depending on an initial void size, that is, an initial condition. A FE model including water desorption was used to verify the conditions for void formation, which could be applied to properly modify the resin curing cycle to avoid or at least reduce porosity.

This study highlights the complexity of accurately predicting void formation in epoxy resins and suggests

the need to further refine the existing models to account for the dynamic interactions between resin chemistry, processing conditions, and environmental factors. Additionally, compared with neat resin, in composite materials, the assumption of spherical voids is unrealistic due to heterogeneous rather than homogeneous nucleation. For these reasons, growth models and curing models remain valid to define the minimum autoclave pressure required to avoid the potential formation of porosity, on the base of thermodynamic considerations.

## AUTHOR CONTRIBUTIONS

**Alfonso Maffezzoli, Francesca Lionetto, and Andrea Dei Sommi:** Conception and design of the study. **Andrea Dei Sommi, Francesca Lionetto, and Giuseppe Buccoliero:** Acquisition of data. **Alfonso Maffezzoli, Francesca Lionetto, Andrea Dei Sommi, and Giuseppe Buccoliero:** Analysis and/or interpretation of data. **Andrea Dei Sommi, Francesca Lionetto, and Alfonso Maffezzoli:** Drafting the manuscript. **Alfonso Maffezzoli, Francesca Lionetto, and Andrea Dei Sommi:** Revising the manuscript. **Andrea Dei Sommi, Francesca Lionetto, Giuseppe Buccoliero, and Alfonso Maffezzoli:** Approval of the version of the manuscript to be published.

## ACKNOWLEDGMENT

Open access publishing facilitated by Universita del Salento, as part of the Wiley - CRUI-CARE agreement.

## CONFLICT OF INTEREST STATEMENT

The authors declare no conflicts of interest.

## DATA AVAILABILITY STATEMENT

Data available on request.

## ORCID

Francesca Lionetto  <https://orcid.org/0000-0003-4466-1161>

Alfonso Maffezzoli  <https://orcid.org/0000-0002-6371-4030>

## REFERENCES

- Jin FL, Li X, Park SJ. Synthesis and application of epoxy resins: a review. *J Ind Eng Chem*. 2015;29:1-11. doi:10.1016/J.JIEC.2015.03.026
- Mohan P. A critical review: the modification, properties, and applications of epoxy resins. *Polym-Plast Technol Eng*. 2013; 52(2):107-125. doi:10.1080/03602559.2012.727057
- Rajak DK, Pagar DD, Menezes PL, Linul E. Fiber-reinforced polymer composites: manufacturing, properties, and applications. *Polymers (Basel)*. 2019;11(10):1667. doi:10.3390/POLYM11101667
- Fleischer J, Teti R, Lanza G, Mativenga P, Möhring HC, Caggiano A. Composite materials parts manufacturing.

- CIRP Ann Manuf Technol.* 2018;67(2):603-626. doi:[10.1016/J.CIRP.2018.05.005](https://doi.org/10.1016/J.CIRP.2018.05.005)
5. Centea T, Grunenfelder LK, Nutt SR. A review of out-of-autoclave prepregs—material properties, process phenomena, and manufacturing considerations. *Compos Part A: Appl Sci Manuf.* 2015;70:132-154. doi:[10.1016/J.COMPOSITESA.2014.09.029](https://doi.org/10.1016/J.COMPOSITESA.2014.09.029)
  6. Hu W, Centea T, Nutt S. Mechanisms of inter-ply void formation during vacuum bag-only cure of woven prepregs. *Polym Compos.* 2020;41(5):1785-1795. doi:[10.1002/PC.25497](https://doi.org/10.1002/PC.25497)
  7. Dei Sommi A, Lionetto F, Maffezzoli A. An overview of the measurement of permeability of composite reinforcements. *Polymers (Basel).* 2023;15(3):728. doi:[10.3390/POLYM15030728](https://doi.org/10.3390/POLYM15030728)
  8. Lionetto F, Moscatello A, Totaro G, Raffone M, Maffezzoli A. Experimental and numerical study of vacuum resin infusion of stiffened carbon fiber reinforced panels. *Materials.* 2020;13(21):4800. doi:[10.3390/ma13214800](https://doi.org/10.3390/ma13214800). [Correction added on 13 August 2024, after first online publication: The journal name of reference 8 has been updated.]
  9. Janzen JP, May D. Solid epoxy prepregs with patterned resin distribution: influence of pattern and process parameters on part quality in vacuum-bag-only processing. *Polym Compos.* 2023;44(11):8153-8167. doi:[10.1002/PC.27696](https://doi.org/10.1002/PC.27696)
  10. Korkees F. Moisture absorption behavior and diffusion characteristics of continuous carbon fiber reinforced epoxy composites: a review. *Polym-Plast Technol and Mater.* 2023;62(14):1789-1822. doi:[10.1080/25740881.2023.2234461](https://doi.org/10.1080/25740881.2023.2234461)
  11. Gillet C, Tamssaouet F, Hassoune-Rhabbour B, Tchalla T, Nassiet V. Parameters influencing moisture diffusion in epoxy-based materials during hygrothermal ageing—a review by statistical analysis. *Polymers (Basel).* 2022;14(14):2832. doi:[10.3390/POLYM14142832/S1](https://doi.org/10.3390/POLYM14142832/S1)
  12. Mehdikhani M, Gorbatiikh L, Verpoest I, Lomov SV. Voids in fiber-reinforced polymer composites: a review on their formation, characteristics, and effects on mechanical performance. *J Compos Mater.* 2019;53(12):1579-1669. doi:[10.1177/0021998318772152/ASSET/IMAGES/LARGE/10.1177\\_0021998318772152-FIG2.JPEG](https://doi.org/10.1177/0021998318772152/ASSET/IMAGES/LARGE/10.1177_0021998318772152-FIG2.JPEG)
  13. Fernlund G, Wells J, Fahrang L, Kay J, Poursartip A. Causes and remedies for porosity in composite manufacturing. *IOP Conf Ser: Mater Sci Eng.* 2016;139:012002. doi:[10.1088/1757-899X/139/1/012002](https://doi.org/10.1088/1757-899X/139/1/012002)
  14. Grunenfelder LK, Nutt SR. Void formation in composite prepregs—effect of dissolved moisture. *Compos Sci Technol.* 2010;16(70):2304-2309. doi:[10.1016/J.COMPSCITECH.2010.09.009](https://doi.org/10.1016/J.COMPSCITECH.2010.09.009)
  15. Stadler H, Kiss P, Stadlbauer W, Plank B, Burgstaller C. Influence of consolidating process on the properties of composites from thermosetting carbon fiber reinforced tapes. *Polym Compos.* 2022;43(7):4268-4279. doi:[10.1002/PC.26687](https://doi.org/10.1002/PC.26687)
  16. Liu L, Zhang BM, Wang DF, Wu ZJ. Effects of cure cycles on void content and mechanical properties of composite laminates. *Compos Struct.* 2006;73(3):303-309. doi:[10.1016/J.COMPSTRUCT.2005.02.001](https://doi.org/10.1016/J.COMPSTRUCT.2005.02.001)
  17. Mujahid Y, Sallih N, Abdullah MZ, Mustapha M. Effects of processing parameters for vacuum-bag-only method on void content and mechanical properties of laminated composites. *Polym Compos.* 2021;42(2):567-582. doi:[10.1002/PC.25848](https://doi.org/10.1002/PC.25848)
  18. Zhang A, Lu H, Zhang D. Research on the mechanical properties prediction of carbon/epoxy composite laminates with different void contents. *Polym Compos.* 2016;37(1):14-20. doi:[10.1002/PC.23149](https://doi.org/10.1002/PC.23149)
  19. Slange TK, Warnet LL, Grouve WJB, Akkerman R. Deconsolidation of C/PEEK blanks: on the role of prepreg, blank manufacturing method and conditioning. *Compos Part A: Appl Sci Manuf.* 2018;113:189-199. doi:[10.1016/J.COMPOSITESA.2018.06.034](https://doi.org/10.1016/J.COMPOSITESA.2018.06.034)
  20. Mamalis D, Floreani C, Brádaigh CMÓ. Influence of hygrothermal ageing on the mechanical properties of unidirectional carbon fibre reinforced powder epoxy composites. *Compos B: Eng.* 2021;225:109281. doi:[10.1016/J.COMPOSITESB.2021.109281](https://doi.org/10.1016/J.COMPOSITESB.2021.109281)
  21. Tretiak I, Kawashita LF, Hallett SR. Manufacturing composite laminates with controlled void content through process control. *J Reinf Plast Compos.* 2024;43(1-2):16-29. doi:[10.1177/07316844231154585/ASSET/IMAGES/LARGE/10.1177\\_07316844231154585-FIG11.JPEG](https://doi.org/10.1177/07316844231154585/ASSET/IMAGES/LARGE/10.1177_07316844231154585-FIG11.JPEG)
  22. Kang C, Zhan J, Ye S, et al. Void stability process window and parametric optimization for filament-wound composite riser. *Polym Compos.* 2024;45(6):5590-5606. doi:[10.1002/PC.28150](https://doi.org/10.1002/PC.28150)
  23. Dei Sommi A, Buccoliero G, Lionetto F, De Pascalis F, Nacucchi M, Maffezzoli A. A finite element model for the prediction of porosity in autoclave cured composites. *Compos B: Eng.* 2023;264:110882. doi:[10.1016/J.COMPOSITESB.2023.110882](https://doi.org/10.1016/J.COMPOSITESB.2023.110882)
  24. Zegeye AD, Delele MA, Tsegaw AA, Bogale TS. Characterization of the void content and laminate quality of fiber-reinforced plastic composites manufactured using the resin spray and compaction method. *Polym Compos.* 2024;45(2):1300-1315. doi:[10.1002/PC.27855](https://doi.org/10.1002/PC.27855)
  25. LeBel F, Ruiz É, Trochu F. Void content analysis and processing issues to minimize defects in liquid composite molding. *Polym Compos.* 2019;40(1):109-120. doi:[10.1002/PC.24609](https://doi.org/10.1002/PC.24609)
  26. Lionetto F, Montagna F, Natali D, De Pascalis F, Nacucchi M, Caretto F. Correlation between elastic properties and morphology in short fiber composites by X-ray computed micro-tomography. *Compos Part A: Appl Sci Manuf.* 2021;140:106169. doi:[10.1016/J.COMPOSITESA.2020.106169](https://doi.org/10.1016/J.COMPOSITESA.2020.106169)
  27. De Pascalis F, Lionetto F, Maffezzoli A, Nacucchi M. A general approach to calculate the stiffness tensor of short-fiber composites using the fabric tensor determined by X-ray computed tomography. *Polym Compos.* 2022;44(2):917-931. doi:[10.1002/PC.27143](https://doi.org/10.1002/PC.27143)
  28. Epstein PS, Plesset MS. On the stability of gas bubbles in liquid-gas solutions. *J Chem Phys.* 1950;18(11):1505-1509. doi:[10.1063/1.1747520](https://doi.org/10.1063/1.1747520)
  29. Amon M, Denson CD. A study of the dynamics of foam growth: analysis of the growth of closely spaced spherical bubbles. *Polym Eng Sci.* 1984;24(13):1026-1034. doi:[10.1002/PEN.760241306](https://doi.org/10.1002/PEN.760241306)
  30. Arefmanesh A, Advani SG, Michaelides EE. An accurate numerical solution for mass diffusion-induced bubble growth in viscous liquids containing limited dissolved gas. *Int J Heat Mass Transf.* 1992;35(7):1711-1722. doi:[10.1016/0017-9310\(92\)90141-E](https://doi.org/10.1016/0017-9310(92)90141-E)
  31. Arefmanesh A, Advani SG. Nonisothermal bubble growth in polymeric foams. *Polym Eng Sci.* 1995;35(3):252-260. doi:[10.1002/PEN.760350306](https://doi.org/10.1002/PEN.760350306)
  32. Roychowdhury S, Gillespie JW Jr, Advani SG. Volatile-induced void formation in amorphous thermoplastic polymeric materials: I. Modeling and parametric studies. *J Compos Mater.* 2001;35(4):340-366. doi:[10.1177/002199801772662208](https://doi.org/10.1177/002199801772662208)
  33. Kardos JL, Duduković MP, Dave R. Void growth and resin transport during processing of thermosetting—matrix composites. In: Dušek K, ed. *Epoxy Resins and Composites IV. Advances in Polymer Science.* Vol 80. Springer; 1986:101-123. doi:[10.1007/3-540-16423-5\\_13](https://doi.org/10.1007/3-540-16423-5_13)

34. Brand RA, Brown GG, Mc Kague EL. Processing science of epoxy resin composites. Air Force Materials Laboratory Report, AFWAL-TR-83-4124. 1984.
35. Boey FYC, Lye SW. Void reduction in autoclave processing of thermoset composites: part 1: high pressure effects on void reduction. *Composites*. 1992;23(4):261-265. doi:10.1016/0010-4361(92)90186-X
36. Wood JR, Bader MG. Void control for polymer-matrix composites (1): theoretical and experimental methods for determining the growth and collapse of gas bubbles. *Compos Manuf*. 1994; 5(3):139-147. doi:10.1016/0956-7143(94)90023-X
37. Gu Y, Li M, Zhang Z, Sun Z. Void formation model and measuring method of void formation condition during hot pressing process. *Polym Compos*. 2010;31(9):1562-1571. doi:10.1002/PC.20944
38. Rengaraj K. *Void Growth Mitigation in High Heating Rate Out-of-Autoclave Processing of Composites*. PhD Thesis. University of Nottingham, 2016.
39. Ledru Y, Bernhart G, Piquet R, Schmidt F, Michel L. Coupled visco-mechanical and diffusion void growth modelling during composite curing. *Compos Sci Technol*. 2010;70(15):2139-2145. doi:10.1016/J.COMPSCITECH.2010.08.013
40. Wang Q, Li T, Wang B, Liu C, Huang Q, Ren M. Prediction of void growth and fiber volume fraction based on filament winding process mechanics. *Compos Struct*. 2020;246:112432. doi:10.1016/J.COMPSTRUCT.2020.112432
41. Sul IH, Youn JR, Song YS. Bubble development in a polymeric resin under vacuum. *Polym Eng Sci*. 2012;52(8):1733-1739. doi:10.1002/PEN.23112
42. Anderson JP, Altan MC. Formation of voids in composite laminates: coupled effect of moisture content and processing pressure. *Polym Compos*. 2015;36(2):376-384. doi:10.1002/PC.22952
43. de Parscau du Plessix B, Le Corre S, Jacquemin F, Lefebure P, Sobotka V. Improved simplified approach for the prediction of porosity growth during the curing of composites parts. *Compos Part A: Appl Sci Manuf*. 2016;90:549-558. doi:10.1016/J.COMPOSITESA.2016.08.024
44. Kermani NN, Simacek P, Advani SG. Porosity predictions during co-cure of honeycomb core prepreg sandwich structures. *Compos Part A: Appl Sci Manuf*. 2020;132:105824. doi:10.1016/J.COMPOSITESA.2020.105824
45. D792 Standard Test Methods for Density and Specific Gravity (Relative Density) of Plastics by Displacement. Accessed March 12, 2024, <https://www.astm.org/d0792-20.html>
46. Karkanis PI, Partridge IK, Attwood D. Modelling the cure of a commercial epoxy resin for applications in resin transfer Moulding. *Polym Int*. 1996;41:183-191. doi:10.1002/(SICI)1097-0126(199610)41:2
47. Lionetto F, Moscatello A, Maffezzoli A. Effect of binder powders added to carbon fiber reinforcements on the chemoreology of an epoxy resin for composites. *Compos B: Eng*. 2017;112:243-250. doi:10.1016/J.COMPOSITESB.2016.12.031
48. Nikishkov Y, Airoldi L, Makeev A. Measurement of voids in composites by x-ray computed tomography. *Compos Sci Technol*. 2013;89:89-97. doi:10.1016/J.COMPSCITECH.2013.09.019
49. Hernández S, Sket F, González C, Llorca J. Optimization of curing cycle in carbon fiber-reinforced laminates: void distribution and mechanical properties. *Compos Sci Technol*. 2013;85: 73-82. doi:10.1016/J.COMPSCITECH.2013.06.005
50. Mehdikhani M, Straumit I, Gorbatiikh L, Lomov SV. Detailed characterization of voids in multidirectional carbon fiber/epoxy composite laminates using x-ray micro-computed tomography. *Compos Part A: Appl Sci Manuf*. 2019;125:105532. doi:10.1016/J.COMPOSITESA.2019.105532
51. Huggins ML. Theory of solutions of high polymers. *J Am Chem Soc*. 1942;64(7):1712-1719. doi:10.1021/JA01259A068/ASSET/JA01259A068.FP.PNG\_V03
52. Online Materials Information Resource–MatWeb. Accessed February 26, 2024, <https://www.matweb.com/index.aspx>
53. Fick AV. On liquid diffusion. *The London, Edinburgh, and Dublin Philosophical Magazine and Journal of Science*. 1855;10(63): 30-39. doi:10.1080/14786445508641925

**How to cite this article:** Dei Sommi A, Lionetto F, Buccoliero G, Maffezzoli A. The effect of absorbed moisture and resin pressure on porosity in autoclave cured epoxy resin. *Polym Compos*. 2024;1-11. doi:10.1002/pc.28870